Fig. 4 gives the experimental impulse response $Q_{A1}(t)$ (Fig. 4*b*) to a single pulse at $t = 0$ on $Q_{B1}(t)$ (Fig. 4*a*) and is compared with theory (Fig. 4*c*) for the device E513Q. Only one pulse over four is significant since, first, to ensure a good repartition of the charge one electrode over two is dummy and secondly the theoretical clock delay is actually of two elementary delays.

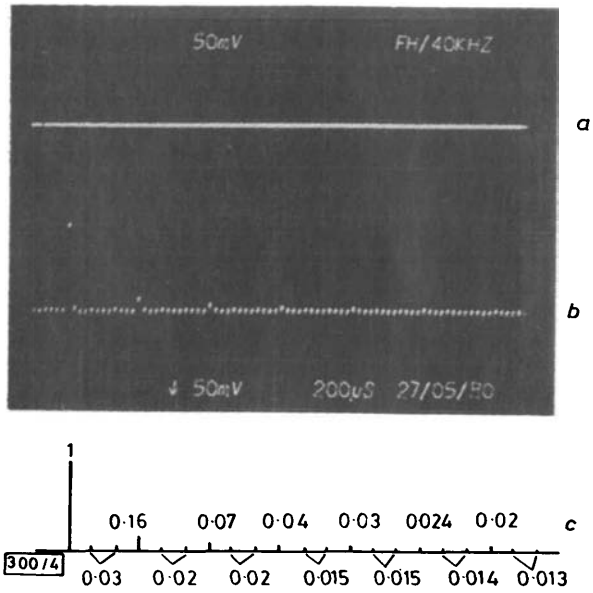

Fig. 4 *Impulse response of E5130 at output diode*
a input pulse
b experimental i.r.
c theoretical i.r.

Fig. 4 demonstrates a very good agreement between calculated and observed impulse responses for a clock frequency F_c equal to 40 kHz but similar results were obtained with measurements performed for F varying from 5 kHz to 500 kHz. This clearly proves the accurate transfer between the two tracks.

In conclusion, we have described a new recursive architecture of a fully integrated filter which overcomes the shortcomings of both transversal charge transfer filters and switched-capacitor filters. Recent progress in the synthesis procedure has shown that the codec filter specifications can be met with a low number of bridges, even when accounting for the 60 Hz notch. Due to passivity, the dynamic range and the stability of this structure are expected to be exceptionally good. Finally, this is a new credible solution for integrated filters in digital communications.

Acknowledgment: The authors would like to thank J.-E. Picquendar, director in charge of Advanced Devices, and M. Blamoutier, J.-L. Berger and A. Vidal at Thomson-CSF, Components and Tubes Group, for their technical assistance in the processing of the silicon wafers.

M. FELDMANN
J. HENAFF
CNET-PAB
Division DTS, Département MAE
921131 Issy-les-Moulineaux, France

17th June 1980

References

1 SMITH, D. A., PUCKETTE, C. M., and BUTLER, W. J.: 'Active bandpass filtering with bucket brigade delay lines', *IEEE J. Solid-State Circ.*, 1972, SC-7, pp. 421–425
2 ENGELER, W. E., TIEMANN, J. J., BAERTSCH, R. D., and GOLDBERG, H. S.: 'A charge transfer recursive filter'; also TIEMANN, J. J., VOGELSONG, T. L., and STECKL, A. J.: 'Charge domain recursive filters'. Papers presented at Int. Symp. Solid-State Circuits Conf., Dig. Tech. Papers, (San Francisco, Ca.), 1980, pp. 154–155, 96–97
3 BOUNDEN, J. E., and TOMLINSON, M. J.: 'C.C.D. Chebyshev filter for radar m.t.i. applications', *Electron. Lett.*, 1974, **10**, pp. 89–90
4 KLAR, H., MAUTHE, M., PFLEIDERER, H. J., POENISCH, O., and KÜNEMAND, F.: 'Passive recursive CCD filters, part I: gasic circuit configuration'; also SCHREIBER, R., BARDL, A., BETZL, H., FEIL, M., and KÜNEMUND, F.: 'Passive recursive CCD filters, part II: gandselect filters'. Papers presented at Int. Symp. Circuits and Systems, IEEE cat. CH 1564, 1980, pp. 1039–1040, 1041–1042
5 GERSHO, A., and GOPINATH, B.: 'Charge-routing networks', *IEEE Trans.*, 1980, **CAS-26**, pp. 81–92
6 FELDMANN, M., and HÉNAFF, J.: French patents 78-19829 (1978) and 79-05108 (1979)

0013-5194/80/150585-03$1.50/0

PICOSECOND PULSE GENERATION IN SEMICONDUCTOR LASERS USING RESONANCE OSCILLATION

Indexing terms: Pulse generators, Lasers, Oscillation

Narrow pulses below 100 ps (f.w.h.m.) have been generated by applying 100 or 300 ps current pulses to a wide-stripe double heterostructure laser. The modulation current was increased to minimise the pulse width.

Introduction: Picosecond pulse generation combined with optical multiplexing is one method to overcome the difficulty of utilising the large optical bandwidths of semiconductor lasers. Mode-locking techniques using semiconductor lasers have recently produced very narrow pulses.[1] Picosecond optical pulse generation from an r.f. modulated AlGaAs diode laser has been reported.[2] In this letter we will report on another method using the first relaxation oscillation pulse of a semiconductor laser when the laser is driven with a modulated current far above threshold.

Experimental considerations: The laser used in this experiment was an LCW-10 broad-stripe laser from Laser Laboratories Inc. The laser was modulated by 100 ps or 300 ps pulses generated from a step recovery diode.[3] The mounting of the laser as well as the pulse generator was made in a microstrip line, and tests showed that the circuit interaction was not important below 6 GHz. The light pulses were detected by a Philco-Ford L 4501 *p-i-n* detector and a sampling oscilloscope. In order to improve the speed of the detector, we loaded it with 11 Ω, which together with the 1·5 pF junction capacitance of the diode should give an *RC* bandwidth of more than 9 GHz.[4] However, a time domain reflectometry measurement showed that the mounting of the detector decreases the bandwidth to about 6 GHz.

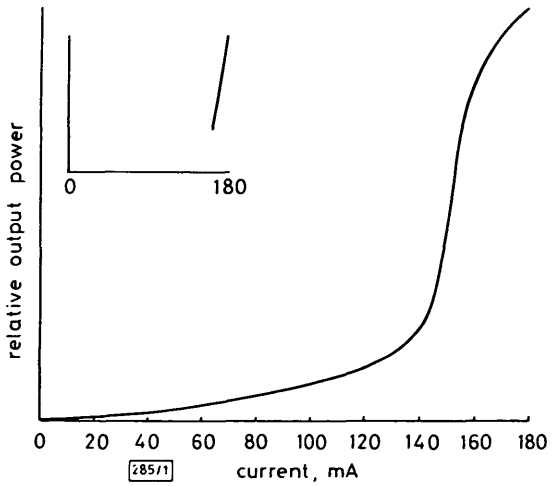

Fig. 1 *Light/current characteristics under d.c. operation. Inset, under pulsed operation*

In Fig. 1 the light/current characteristics of the laser are shown. The d.c. current was slowly swept from zero to 180 mA, which corresponds to 40 mA above threshold. The curve shows typical characteristics of a broad-stripe laser. It is fairly linear in the region of 142 to 155 mA, and then saturation due to increased optical losses and heating occurs. The linear region is considerably wider if the light/current characteristics are measured during pulsed operation as shown in the inset of Fig. 1. The laser is modulated with a 300 ps wide pulse. The variable pulse current, from 10 to 30 mA, was superimposed on a bias current of 152 mA.

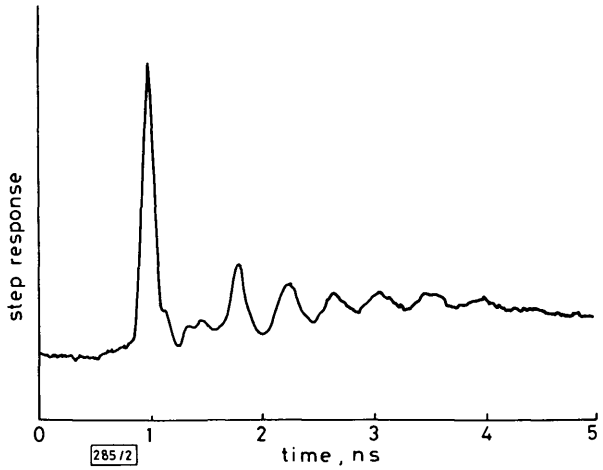

Fig. 2 *Step response of laser; bias current 125 mA, step current 42 mA*

The step response of the laser diode is shown in Fig. 2. The d.c. bias was 125 mA and the step current 42 mA. The input rise time was measured to be 300 ps. Typical relaxation oscillation behaviour is illustrated in the Figure. In our particular experiment the relaxation oscillation frequency measured between the first two peaks is 1·2 GHz, and 2·3 GHz when measured between the second peaks. The relaxation frequency can be approximated from the linearised rate equations to be

$$f_r = \frac{1}{2\pi}\left[\frac{1}{\tau_p \tau_e}\left(\frac{I}{I_{th}} - 1\right)\right]^{1/2} \quad (1)$$

where τ_p and τ_e are the photon and electron lifetimes, respectively, I is the drive current and I_{th} is the threshold current. It is evident that the resonance frequency increases with higher drive current and consequently the width of the first relaxation pulse generated will be narrower. The difference in resonance frequency, when measured between the first or the second peaks in the step response, is probably due to the broadening of the transverse mode on a more lossy region. This causes the photon lifetime to decrease and hence the resonance frequency to increase.[5]

A Gaussian 100 ps wide input pulse is shown in Fig. 3*a*. The output light pulse observed at the detector has f.w.h.m. of 100 ps as shown in Fig. 3*b*. The true pulse waveform, which has been corrected for the 6 GHz bandwidth limitation of the detector, is shown dotted in the Figure. The width of the pulse was found to be 85 ps. The d.c. bias of the diode was set at approximately 10 mA above threshold. This was found to be the optimum bias value for the maximum pulse height. With a pulse current of 140 mA the lowest pulse width (85 ps) was obtained. When a 300 ps wide pulse current was used as shown in Fig. 3*c*, the output light pulse became almost as narrow as in the 100 ps case, though for a lower pulse current. An 80 mA input pulse current resulted in a 95 ps wide output light pulse, as can be seen in Fig. 3*d*.

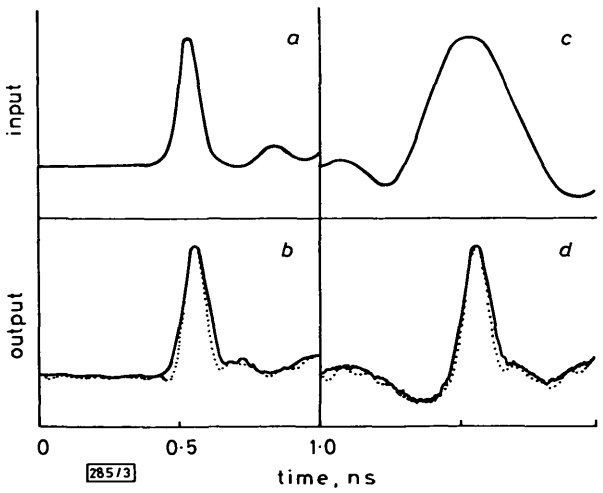

Fig. 3

a 100 ps input pulse
b Optical output from 100 ps wide, 140 mA high input pulse
c 300 ps input pulse
d Optical output from 300 ps wide, 80 mA high input pulse

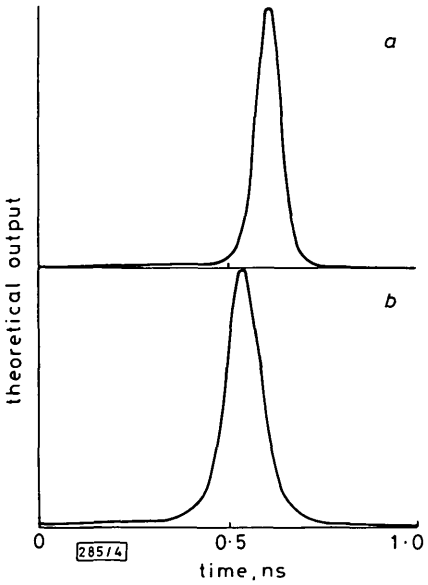

Fig. 4

a Calculated optical output pulse for 100 ps wide input pulse
b Calculated optical pulse for 300 ps wide input pulse

A computer solution of the rate equations is shown in Fig. 4. The simple single-mode equations without carrier diffusion but including spontaneous emission was employed.[6] The theoretical output pulses with 100 and 300 ps input pulses are shown in Fig. 3*a* and 3*b*, respectively. The computer model of the laser does seem to give an adequate explanation of the phenomena observed since the theoretical results conform very well with the experimental data.

Conclusions: A simple method based upon the resonance oscillation phenomenon in semiconductor lasers has been found to generate picosecond pulses, useful for, e.g., characterising Gbit/s photodetectors and dispersion measurements of single-mode and multimode fibres. By using optical multiplexing, these pulses can be used for very high data rate optical fibre transmission systems.

P. TORPHAMMAR
S. T. ENG

Department of Electrical Measurements
Chalmers University of Technology
S-412 96 Göteborg, Sweden

13th June 1980

References

1 HO, P.-T., GLASSER, L. A., IPPEN, E. P., and HANS, H. A.: 'Picosecond pulse generation with a c.w. GaAlAs laser diode', *Appl. Phys. Lett.*, 1978, **33**, pp. 241–242
2 ITO, H., YOKOYAMA, H., MURATA, S., and INABA, H.: 'Picosecond optical pulse generation from an r.f. modulated AlGaAs d.h. diode laser', *Electron. Lett.*, 1979, **15**, pp. 738–740
3 TELL, R., TORPHAMMAR, P., and ENG, S. T.: 'Multiplexer at 5 Gbit/s for fibre-optical communication systems', *ibid.*, 1977, **13**, pp. 765–766

4 ANDERSSON, T., and ENG, S. T.: 'Gigahertz bandwidth measurements of photodetectors and fibers using picosecond pulses generated by semiconductor lasers', unpublished
5 DIXON, R. W., JOYCE, W. B., and MILLER, R. R.: 'On the relationship of light-output nonlinearities and light-output spikes in proton-bombarded stripe-geometry double-heterostructure (Al, Ga)As lasers', *J. Appl. Phys.*, 1979, **50**, pp. 1128–1130
6 TORPHAMMAR, P., TELL, R., EKLUND, H., and JOHNSTON, A. R.: 'Minimizing pattern effects in semiconductor lasers at high rate pulse modulation', *IEEE J. Quantum Electron.*, 1979, **QE-15**, pp. 1271–1276

0013-5194/80/150587-03$1.50/0

IMPROVED DIGITAL AUTOMATIC GAIN CONTROL FOR P.C.M. SIGNALS

Indexing terms: Digital transmission, Pulse-code modulation

A digital automatic gain control is described which uses an open-loop instead of a closed-loop configuration. This change has been made to eliminate oscillations in gain which occurred with sinusoidal input signals in the closed-loop system described previously. Results of a computer simulation of the new system are presented.

In a recent letter,[1] the authors described a digital automatic gain control (d.a.g.c.) for processing 30 p.c.m. channels. This system used a closed-loop configuration. During subsequent testing, it was found that, although operation was satisfactory on speech signals, the gain sometimes oscillated when sinusoid signals were transmitted.[2] These oscillations occurred for a different range of input levels for input signals of different frequencies. They happened because a sinusoidal signal has a different distribution of voltage with time from a speech signal. The normal range of operation, which was 6 dB on speech, corresponded to only 1 dB for a sinewave. Consequently, the system never reached equilibrium. To eliminate this problem, the system was redesigned to use an open-loop configuration.

The earlier system provided 4 gain settings (−6 dB, 0 dB, 6 dB, 12 dB) and operated by comparing the output level with two reference levels separated by 6 dB. The modified system compares the input signal with 3 reference levels and sets the gain accordingly. As before, the system operates by counting the number of input samples N which are above a threshold level λ_1 during a time period T. Thus, the actions performed are:

If $N \leq N_1$ insert 12 dB gain
If $N_1 < N \leq N_2$ insert 6 dB gain
If $N_2 < N \leq N_3$ insert 0 dB gain
If $N_3 < N$ insert 6 dB loss,

where $N_1 < N_2 < N_3$. This system was simpler to implement than the alternative having a single range for N and 3 different thresholds.

A block diagram of the modified d.a.g.c. is shown in Fig. 1. The p.r.o.m contains a look-up table for the appropriate 8-digit output word for every input word for each of the gain settings. Each address is selected by a 10-bit word, which comprises 8 bits from an incoming p.c.m. sample and two bits (S_1 and S_2) corresponding to the gain control for that channel. The incoming p.c.m. signal is converted from serial to parallel mode before processing and the output signal is converted back to serial mode, as shown in Fig. 1. It is also necessary to arrange for the digits contained in time slots 0 and 16 (which are used for frame alignment and signalling, respectively) to bypass the signal processing system. This is not shown in Fig. 1. To prevent pauses in speech being considered as low-level speech and so causing maximum gain to be inserted, a speech detector is used. The magnitude of each incoming sample is compared with a second threshold level λ_2 which was chosen to be 40 dB below the limiting level. Thus, excluding the sign digit, $\lambda_2 = 0010100$.

The samples whose magnitudes exceed λ_1 are detected by a digital comparator C_1, and those below λ_2 are detected by C_2. The comparators are connected to logic units LU1 and LU2, respectively. Each sample exceeding the threshold causes the LU to add '1' to the count stored for that channel in a shift register. This operates in synchronism with the p.c.m. system and presents its contents for each channel in turn to the logic units LU1, 2 and 3. For each channel it stores: the number of samples exceeding λ_1 (processed by LU1), the number of samples exceeding λ_2 (processed by LU2) and the gain control digits S_1, S_2 (processed by LU3). When the number of active samples exceeding λ_2 (determined by comparator C_6) which

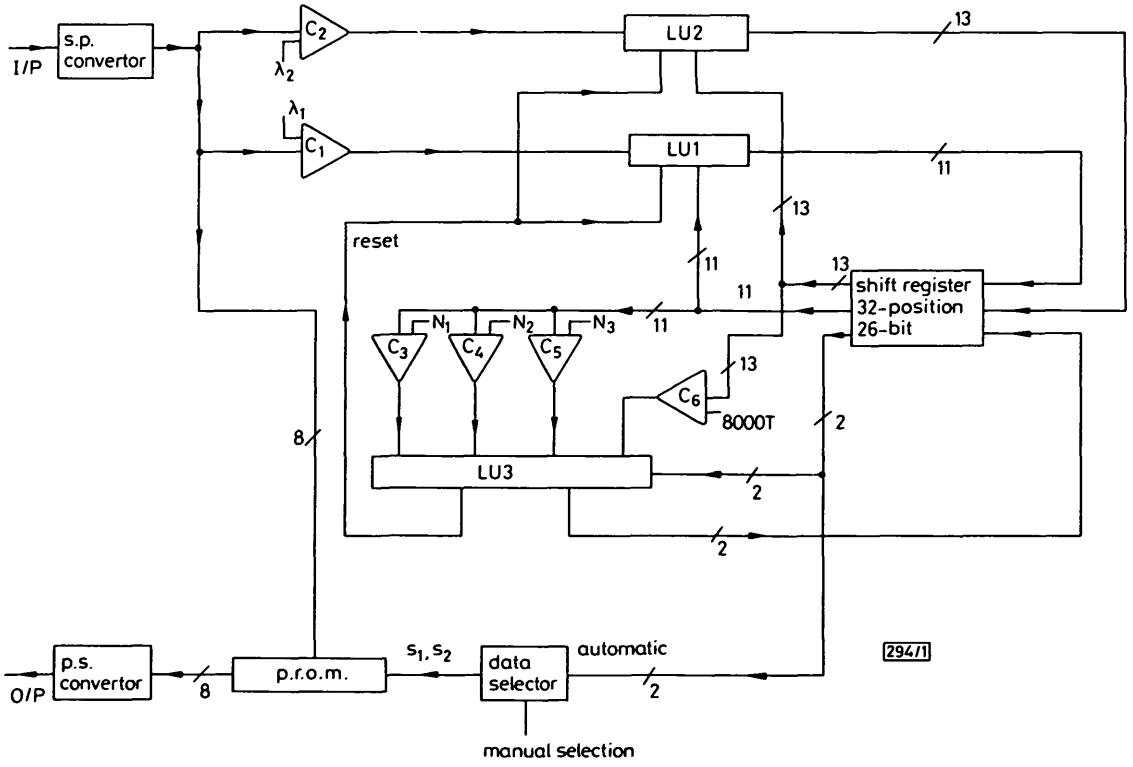

Fig. 1 *Block diagram of d.a.g.c.*